Journal of Chemical Technology and Metallurgy, 51, 5, 2016, 556-562

MORPHOLOGICAL AND CRYSTALLOGRAPHIC CHARACTERISTICS OF ELECTROCHEMICALLY DEPOSITED TERNARY ALLOY ZINC-NICKEL-COBALT

Sasa Micin[1], Sanja Martinez[2], Borislav N. Malinovic[3], Vedrana Grozdanic[4]

[1] *Ekvator Ltd, Karađorđeva 12, 78000 Banja Luka, RS, B&H*
[2] *University of Zagreb Faculty of Chemical Engineering and Technology Zagreb, Republic of Croatia*
[3] *University of Banja Luka, Faculty of Technology Stepe Stepanovica 73, 78000 Banja Luka, RS, B&H E-mail: borislav.malinovic@unibl.rs*
[4] *Center for Material Research of Istrian region METRIS, Zagrebačka 30, 52100 Pula Republic of Croatia*

Received 09 December 2015
Accepted 20 May 2016

ABSTRACT

Morphological and crystallographic characteristics of electrochemically deposited ternary alloy ZnNiCo metal coatings obtained by using different anodes have been investigated using X-ray diffraction and scanning electron microscopy. The dominant phases in the deposited coatings are γ (330) and η - Zn (101) phase. The mean crystallite size is 5,2 nm - 36,2 nm. By the analysis of morphological characteristics the average grain size form 748 to 1147 nm has been determined and shown to increase in order BDD < MMO < Ti/Pt anodes. The investigated coatings may be classified as fine-grained.

Keywords: ternary alloy ZnNiCo, electrodeposition, morphological characteristics, crystallographic characteristics, anode.

INTRODUCTION

Significantl influence on corrosion characteristics of electrochemically deposited metal coatings have morphological and crystallographic features of the deposited sediment. It is known that metallic compact fine-grained deposits show greater corrosion resistance.

In general, the metal precipitates deposited in the high overpotentials and low current density show better characteristics from the standpoint of morphology and crystalline structure and therefore high corrosion resistance [1].

Terms deposition such as chemical composition of the electrolyte, the concentration of metal ions, current density, the materials of the anode influence significantly morphological and crystallographic characteristics of the metal coating and therefore their corrosion characteristics.

In this study we investigated the influence of different dimensionally stable anodes (DSA) on morphological and crystallographic characteristics ternary alloy ZnNiCo coating, electrochemically deposited from chloride electrolyte (bath).

We used anodes made of platinum (Pt), a mixture of metal oxide (MMO) and boron doped diamond (BDD). Besides dimensional stability, an important characteristic of these anodes represents the overpotential for the oxygen evolution reaction (OER) [2 - 8].

EXPERIMENTAL

Electrochemical deposition of ZnNiCo alloy

For electrochemical deposition of ZnNiCo alloy, we used the following laboratory equipment: 600 ml volume laboratory glass, electrolyte, anode, cathode, the DC power supply and necessary ancillary equipment (carriers, cable connections, etc.).The chemical composition of chloride electrolyte used for deposition of coatings of ternary alloy ZnNiCo is shown in Table 1.

Table 1. The chemical composition of the electrolyte used for the deposition of the ternary alloy Zn-Ni-Co.

Component	Molecular mass g/mol	The composition of the electrolyte
$ZnCl_2$	136,315	0,4 M
$NiCl_2$ x $6H_2O$	237,71	0,04 M
$CoCl_2$ x $6H_2O$	237,93	0,04 M
NH_4Cl	53,4915	2,24 M
KCl	74,5513	1,61 M
$C_6H_5Na_3O_7$	258,069	0,034 M

The following types of anodes were used:

● Platinised titanium (Ti/Pt) - The base material of the anode is titanium covered with a layer of platinum in the form of mesh, where the openings (mesh) are Type A (ital. V); manufacturer METAKEM GmbH, Germany (Ti-grade 2; 2,5 μm Pt).

● The mixed metal oxide (MMO) - The coating of mixture of oxides IrO_2 and RuO_2 on titanium surface is in the form of mesh (mesh type A); METAKEM GmbH, Germany.

● Diamond (*boron*-doped diamond - BDD) - coating of diamond is doped with boron on the surface of niobium in the form of mesh (mesh type B); METAKEM GmbH, Germany.

The cathode is made up of commercial steel pickled sheet, (mild steel - EN 10130/91+A1/98), which chemical composition is obtained by AES (atomic emission spectrometer) method using device LECO 500A.

As a source of DC power is used a digital adapter Atten, APS3005SI, 30V, 5A.

Preparation of the electrolyte is performed by using p.a. chemicals and distilled water (4 μS/cm conductivity). The ratio of anode and cathode surface was 2:1. The deposition was performed at room temperature without stirring. Cathodic current density was 3 A/dm^2. Time of deposition is 15 minutes. Preparation of the substartes is performed by mechanical polishing with abrasive paper (label 600, 800, 1200), degreasing in trichloroethylene and pickling with hydrochloric acid (1:1).

Weight, thickness and density of deposited coatings

The mass of the coating was determined by measuring of the weight of the samples before and after deposition by laboratory balances (accurancy ± 0,0001 g).

The thickness of the deposited metal alloy coatings were measured by using magnetic meter "MIKROTEST II/III magnetic coating thickness gauge", type G II, according to DIN 50981 & 50982, manufacturer ELEKTRO-PHYSIK, Germany.

The density of the coating is calculated by using the mass and volume of the coating. The volume is determined from the measured values of the layer thickness and surface area of the layer.

The chemical composition of deposited coatings

The chemical composition of the deposited coatings was determined by energy dispersive spectrometry (EDS method) using the high resolution scanning electron microscope FEG QUANTA 250, manufacturer FEI, USA.

Table 2. Weight, thickness and density of the coating depending on the used anode material.

Used anode material			MMO	Ti/Pt	BDD
The mass of the deposited coatings	m	g	0,1338	0,1625	0,2106
The thickness of the deposited coatings	$\overline{d}$	μm	11,86	13,6	13,99
The density of the deposited coatings	$\rho_{prevlake}$	g cm^{-3}	7,9	6,8	6,3
Cathodic current density	j_{tal}	A/dm^2	3	3	3
The measured voltage of galvanic cell	U	V	2,5	2,6	3,3

X-ray Diffraction

Crystallographic analysis was performed by using the X-ray diffractometer, type APD 2000, manufacturers ItalStructures, Italy. The crystallite size was determined from Scherrer's equation (1):

$$D_{hkl} = \frac{K\lambda}{\beta \cos\theta} \quad (1)$$

where D_{hkl} (Å) - average crystallite size in the direction perpendicular to the array level with which X-rays diffract, K - shape factor (0.9-1), λ - wavelength the X-radiation (1.54056 Å), β - the width of the diffraction maximum measured at mid height of the maximum, θ - Bragg's angle.

The spacing between the crystalline level is determined by using the Bragg's equation (2):

$$\lambda = 2d \sin\theta \quad (2)$$

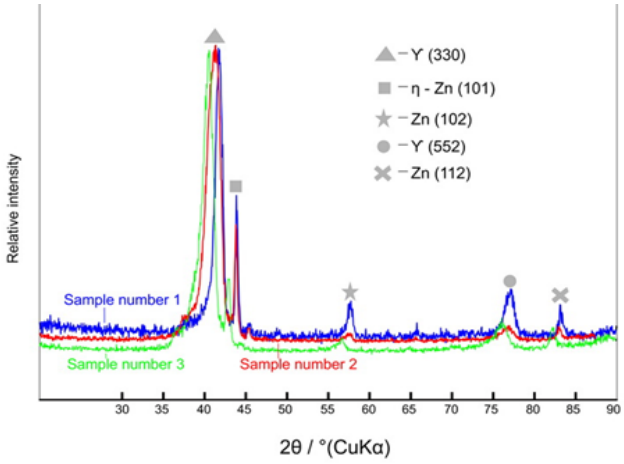

Fig. 1. Diffraction patterns of the samples in spectrum $2\theta=20^0$ - 90^0.

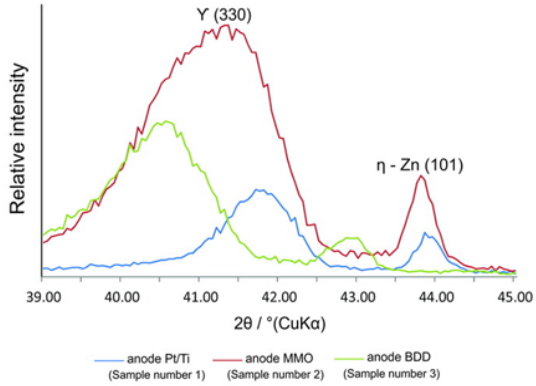

Fig. 2. Diffraction patterns of the samples in spectrum $2\theta = 39^0$- 45^0.

Scanning electron microscopy

Analysis by SEM technique was performed by using the scanning electron microscope high resolutions type FEG QUANTA 250, manufacturer FEI, USA.

RESULTS AND DISCUSSION

Weight, thickness and density of deposited coatings

Weight, thickness and density of electrochemically deposited coatings depending on the used anode material are shown in Table 2.

The values of the voltage of galvanic cell were measured directly from a digital adapter.

The chemical composition of the deposited coatings

The chemical composition of the deposited metal coatings was obtained on many different points. The mean values are shown in Table 3.

Analysis of the results of measurements of the chemical composition of the metal ternary ZnNiCo alloy shows different values at different points of measurement, which indicates the heterogeneity of the deposits in chemical composition.

X-ray Diffraction

Results of the analysis of crystallography structure of deposits are shown in two parallel different widths of the spectrum in order to monitor the peak diffraction patterns. Crystallite size and distance between

Table 3. Mean values of the chemical composition of alloys.

anode element (mas %)	Ti/Pt (Sample no. 1)	MMO (sample no. 2)	BDD (sample no. 3)
Zn	78,87	83,99	89,68
Ni	2,21	1,93	2,21
Co	2,18	1,79	2,19
C	14,78	10,19	4,68
O	1,96	5,55	1,24

equidistant surfaces were determined by Scherrer's and Bragg's equation. Fig. 1 presents an overview diffraction patterns of the samples for the width of the spectrum 2θ = 20^0 - 90^0.

In Fig. 1 can be seen that in all tested samples peaks at values of 2θ = 40,55 to 41,8; 2θ = 42,85 to 43,85; 2θ = 56,75 to 57,57; 2θ = 75,95 to 77,2 and 2θ = 82,3 to 83,1 of different intensity. The peak is corresponding to the most intense γ crystallographic structure (330) phase, where the peaks of Ni_5Zn_{21} or Co_5Zn_{21} coincide. Slightly less intensive the second peak can be attributed to the crystalline phase *η*-Zn (101). Other distinct peaks may be attributed to crystallographic phases of Zn (102), *γ* (552), Zn (112), and they are significantly less intensive compared to the γ phase (330) and *η*-Zn (101).

Fig. 2 presents the number of diffraction patterns with the range of the spectrum, 2θ = 39^0 - 45^0, where most intense peaks occur. Fig. 2 shows that using different anode during deposition of coatings, different values of Brag's angle (2θ) and relative intensity occur.

The coating obtained with Ti/Pt anode, shows the presence of *γ* (330)-phase for value of Bragg's angle 2θ = $41,8^0$ and relative intensity (573) with a value of 44% less than the intensity of diffraction patterns that shows coating obtained with BDD anode and 65 % less than the diffraction patterns of coating obtained by MMO anode. *η* phase - Zn (101) occurs at the value of 2θ = $43,85^0$ and approximately equal intensity (293) with value that gives diffraction pattern of coating formed with BDD anode (258). In relation to the intensity value for the phase *η*-Zn (101) deposited by MMO anode (669), the coating obtained with Ti/Pt anode shows peak intensity decreased by 56 %.

The coating obtained with MMO anodes, shows the presence of *γ* (330) - phase for the angle value of 2θ = $41,35^0$ and *η*-Zn (101) phase for the angle value of 2θ = $43,8^0$. The intensity of the peaks phases has higher values than the other tested samples.

The diffraction pattern of deposit, using BDD anode gives pronounced peaks for the angle value of 2θ = $40,55^0$ (phase *γ* (330)) and 2θ = $42,85^0$ (phase *η*-Zn (101)).

The dominant crystallographic orientation in the structure of the deposited ZnNiCo alloy can be determine by using Muresan's method [9 - 11] by calculating the texture coefficient (*Tc(hkl)*), using the expression (3)[12]:

$$Tc(hkl) = \frac{I(hkl)}{\sum I(hkl)} \times \frac{\sum I_0(hkl)}{I_0(hkl)} \times 100 \qquad (3)$$

where *I(hkl)* - peak intensity of the deposited alloy, Σ *I(hkl)* - the sum of intensities of all independent peaks, $I_0(hkl)$ - peak intensity of the standard diffraction patterns for Zn, Σ $I_0(hkl)$ - the sum of all independent intensity peaks for Zn. The textured coefficient of ternary ZnNiCo alloy coatings is shown in Table 4. Testing the crystalline structure of the deposited double ZnCo alloy has shown that the structure of ZnCo is the same as structure of Zn but with different crystallographic orientations [13].

Crystallographic analysis of binary coating Zn-Ni deposited from chloride bath showed that three main phases in the coating Zn-Ni exist, *α*, *γ* and *η*-phase. *α* represents the phase of the solid solution of Zn and Ni from the equilibrium solubility of about 30 % Zn. *γ*-phase can be defined as an intermediate phase with the composition Ni_5Zn_{21}. *η*-phase is a solid solution of Ni and Zn with a small amount of Ni [14]. The values of 2θ angles for *γ*-phase, composition Ni_5Zn_{21} and *η*-phase Zn (101) of all tested samples are in agreement with literature data [15 - 17].

The diffraction pattern of deposits of the binary Zn-Co alloy obtained from sulfuric acid solution, showed that in the coating *γ* (330)-phase is dominant [18]. Results of Mouanga et al. [12] suggest that the use of chloride electrolyte for deposition of binary Zn-Co alloy lead to formation of dominant *η*-Zn (101) phase.

Experimental results of phase composition of coatings of ternary Zn-Ni-Co alloys, deposited from chloride electrolytes, showed dominant presence of *η*-phase Zn (101) [19, 20], while in the coatings deposited from sulfate solutions the presence of *γ*-phase and Ni_5Zn_{21} is established [21 - 24].

Crystallite size and the distance between the crystal surfaces calculated from Scherer's equation (1) and Brag's equation (2) are shown in Table 5.

The crystallite size ranged from 5,2 nm to 36,2 nm depending on the anode. The results of study on the structure of electrochemically deposited binary ZnCo alloy [18], showed the value of the crystallite size of 26,7 nm to 42,4 nm. The results for electrochemically deposited binary ZnNi alloys showed that the crystallite size is in the range of 20 nm to 50 nm, and with the increase of Ni content in the precipitate, the crystallite size increases [16].

Scanning electron microscopy

Analysis of the morphological characteristics of the deposited coating was performed using scanning electron

Table 4. The textured coating deposited coefficient depending on the used anodes.

Crystallographic orientation, hkl	The textural coefficient, Tc(hkl) %		
	Ti/Pt, (sample no. 1)	MMO, (sample no. 2)	BDD, (sample no. 3)
330	49,7	63,5	66,7
101	25,4	25,5	16,7
102	7,8	2,6	3,8
552	9,8	4,2	7,0
112	7,2	4,0	6,1

microscopy with different magnification (Fig. 3).

It was found analyzing the morphological characteristics of the samples that the average particle size is from 748 to 1147 nm, placing them in the range of fine-particle coatings [25].

The coatings of ternary alloy obtained with MMO anode show the lowest value of the electrochemical cell voltage (2,5 V) and they are characterized by the smallest average size of the particles as well as the highest degree of homogeneity from the standpoint of particle size.

The voltage on the electrochemical cell with Ti/Pt anode is 2,6 V. The average particle size is 1147 nm where the level of homogeneity of the coatings is slightly lower compared to the coatings obtained with MMO anode.

The electrochemical cells with BDD anode show the highest value of voltage (3,3 V) and a minimum value of average size of particles (748 nm).

CONCLUSIONS

On the basis of the presented experimental results on electrochemical deposition of coatings of ternary ZnNiCo alloy, the following conclusions can be drawn:

- The diffraction patterns of all examined samples give reflections for Bragg's angle $2\theta = 40,55^0$ - $41,8^0$; $2\theta = 42,85^0$ - $43,85^0$; $2\theta = 56,75^0$ - $57,57^0$; $2\theta = 75,95^0$ - $77,2^0$ and $2\theta = 82,3^0$ - 83^0.
- The intensity of the peaks varies depending on the chemical composition of the coating or used anode during deposition. The most intense peak values can be related to γ (330) and η-Zn (101) phases.
- The dominant crystallographic orientation is determined by the chemical composition of the metallic coatings.
- The mean value of the crystal size is 5,2 nm - 36,2 nm, depending on the sample and crystalline phases.
- It has been shown that all obtained coatings can be described as fine-particle coatings.
- It is evident that the crystallographic and morphological characteristics of deposits are different. A significant influence on the crystallographic and morphological structure has the chemical composition of deposits.

The influence of anode material on the electrodeposition of metal coatings can be interpreted using the fact that oxygen and other electroactive materials have dif-

Table 5. The crystallite size of sediment deposited using different anode recalculated based on Scherrer's equation and the distance between the crystal surfaces defined on the basis of the Bragg's equation.

Sample No	1 (anode Ti/Pt)		2 (anode MMO)		3 (anode BDD)	
Crystallographic orientation, hkl	Crystallite size	Distance between the crystalline level	Crystallite size	Distance between the crystalline level	Crystallite size	Distance between the crystalline level
330	17,2	0,087	16,2	0,08	36,6	0,078
552	19,9	1,165	19,9	0,846	13,5	0,144
101	11,3	0,136	11,1	0,141	6,4	0,766
112	8,8	0,098	5,2	0,119	5,2	0,283
102	13,1	0,118	12,1	0,135	10,4	0,253

*Crystallite size determined based on Scherrer 's equation (nm),

**Distance between crystal plane Bragg's equation (nm).

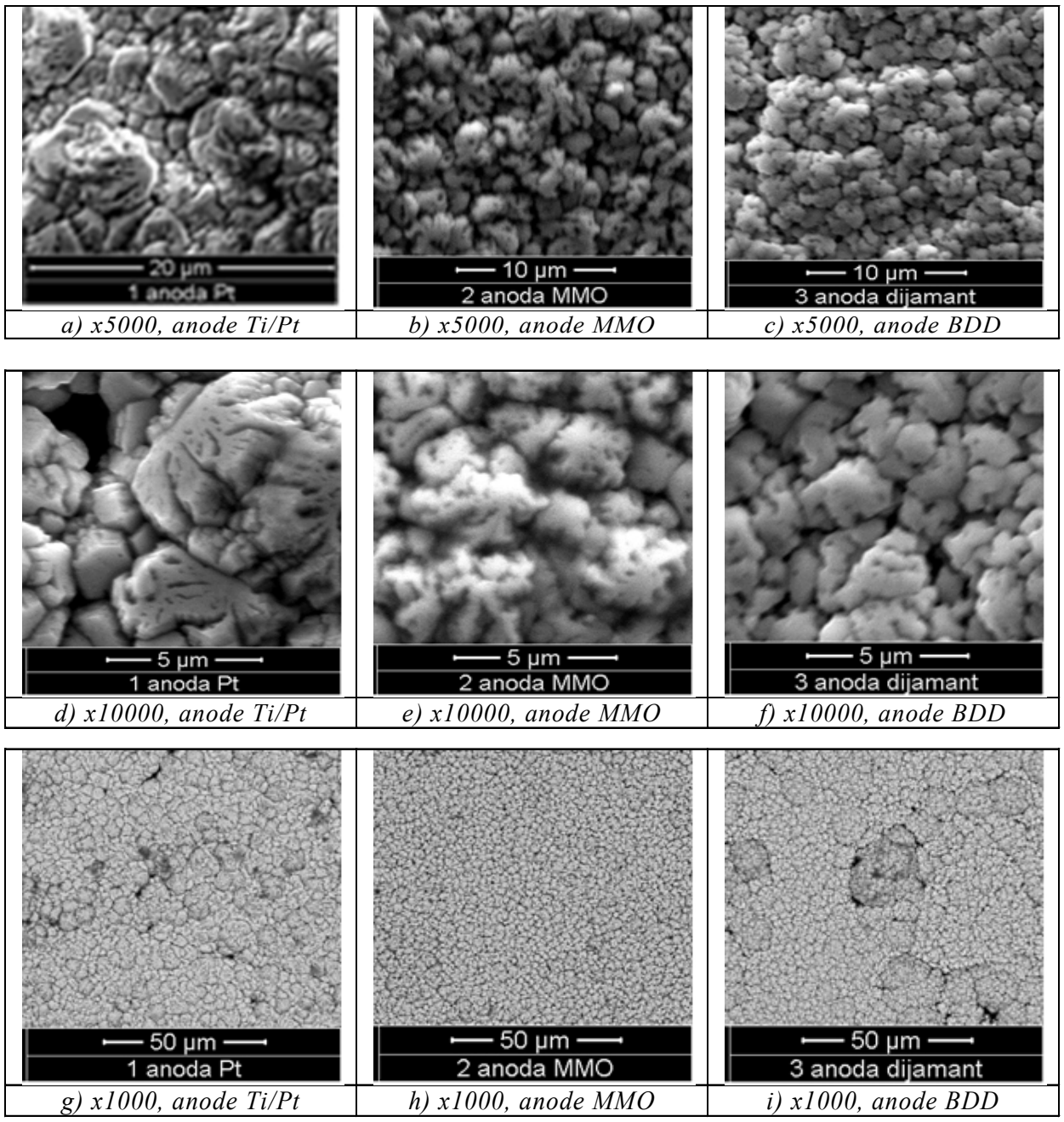

Fig. 3. SEM photos of electrochemically deposited coatings of ternary ZnNiCo alloy obtained with Ti/Pt, MMO and BDD anodes.

ferent oxidation potentials of the various anodes. Due to the potential change of oxidation there is a change of density of partial anodic current and the total anodic current density. Bearing in mind that the current density in an electrochemical cell is constant, change in density of the total anodic current causes a change in the total cathode current density and changes in potential deposition coatings. Due to the change in the total cathode current density leads to depositing coatings of different chemical composition, which show different morphological and crystallographic characteristics.

REFERENCES

1. S. Dordević, M. Maksimović, M. Pavlović, K. Popov, Galvanotehnika, Tehnička knjiga, Beograd 1997, (in Serbian).

2. M. Hamza, R. Abdelhedi, E. Brillas, I. Sirés, Comparative electrochemical degradation of the triphenylmethane dye Methyl Violet with boron-doped diamond and Pt anodes, J. of Electroanalytical Chem., 627, 2009, 41-50.
3. X. Chen, G. Chen, P.L. Yue, Anodic oxidation of dyes at novel Ti/B-diamond electrodes, Chem. Eng. Sci., 58, 2003, 995-1001.
4. M. Fryda, A. Dietz, D. Herrmann, A. Hampel, L. Schäfer, C.-P. Klages, A. Perret, W. Haenni, C. Comninellis, D. Gandini, Wastewater treatment with diamond electrodes, New Diam. Front. C. Technol., 9, 1999, 229-240.
5. J. Chen, H. Shi, J. Lu, Electrochemical treatment of ammonia in wastewater by RuO_2-IrO_2-TiO_2/Ti electrodes, J. Appl. Electrochem., 37, 2007, 1137-1144.
6. Lj. M. Vračar, Amorfne legure kao elektrokatalizatori za anodnu kiseoničnu reakciju, Hem. Ind., 54, 2, 2000, 45-49, (in Serbian).
7. H. Tamura, T. Arikado, H. Yoneyama, Y. Matsuda, Anodic oxidation of potassium cyanide on platinum electrode, Electrochimica Acta, 19, 1974, 273-277.
8. A. Valiūnienė, V. Antanavičius, Ž. Margarian, I. Matulaitienė, G. Valinčius, Electrochemical oxidation of cyanide using platinized Ti electrodes, Materials Sci., 19, 4, 2013, 385-389.
9. P. Fricoteaux, J. Douglade, Texture evolution of electroplated copper under various modes of convection, Effect of dissolved oxygen, J. Mater. Sci. Letters, 21, 2002, 1485-1488.
10. S.H. Kim, H.J. Sohn, Y.W. Kom, T.H. Yim, H.Z. Lee, T. Kang, Effect of saccharin addition on the microstructure of electrodeposited Fe-36 wt % Ni alloy, Surf. Coat. Technol., 199, 2005, 43.
11. R. Ramanauskas, P. Quintana, L. Maldonado, R. Pomés, M.A.P. Canul, Corrosion resistance and microstructure of electrodeposited Zn and Zn alloy coatings, Surf. Coat. Technol., 92, 1997, 16-21.
12. M. Mouanga, L. Ricq, P. Berçot, Electrodeposition and characterization of zinc-cobalt alloy from chloride bath ; influence of coumarin as additive, Surf. & Coat. Technol., 202, 2008, 1645-1651.
13. R. Fratesi, G. Lunazzi, G. Roventi, Organic and Inorganic Coatings for Corrosion Prevention, (Eds. L. Fedrizzi, P.L. Bonora), EFC Publications No 20, The Institute of Materials, London, 1997, p. 130.
14. C. Müller, M. Sarret, M. Benballa, Complexing agents for a Zn-Ni alkaline bath, J. Electroanal. Chem., 519, 2002, 85.
15. Zhi-feng Lin, Xiang-bo Li, Li-kun Xu, Electrodeposition and Corrosion Behavior of Zinc-Nickel Films Obtained From Acid Solutions; Effects of TEOS as Additive, Int. J. Electrochem. Sci., 7, 2012, 12507-12517.
16. R. Rizwan, M. Mehmood, M. Imran, J. Ahmad, M. Aslam, J.I. Akhter, Deposition of Nanocrystalline Zinc-Nickel Alloys by D.C. Plating in Additive Free Chloride Bath, Mater. Trans., 48, 6, 2007, 1558-1565.
17. A. Levesque, S. Chouchane, J. Douglade, R. Rehamnia, J.P. Chopart, Effect of natural and magnetic convection on the structure of electrodeposited zinc-nickel alloy, App. Surf. Sci., 255, 2009, 8048-8053.
18. S. Lichušina, A. Chodosovskaja, A. Sudavičius, R. Juškėnas, D. Bučinskienė, A. Selskis, E. Juzeliūnas, Cobalt-rich Zn-Co alloys: electrochemical deposition, structure and corrosion resistance, Chemija, 19, 1, 2008, 25-31.
19. N. Eliaz, K. Venkatakrishna, A. Chitharanjan Hegde, Electroplating and characterization of Zn-Ni, Zn-Co and Zn-Ni-Co alloys, Surf. Coat. Technol., 205, 2010, 1969-1978.
20. M.M. Younan, Surface microstructure and corrosion resistance of electrodeposited ternary Zn-Ni-Co alloy, J.Appl. Electrochem., 30, 2000, 55-60.
21. M.M. Abou-Krisha, H.M. Rageh, E.A. Matter, Electrochemical studies on the electrodeposited Zn-Ni-Co ternary alloy in different media, Surf. Coat. Techn., 202, 2008, 3739-3746.
22. R.S. Bhat, U.K. Bhat , A.C. Hegde, Corrosion Behavior of Electrodeposited Zn-Ni, Zn-Co and Zn-Ni-Co Alloys, Anal. Bioanal. Electrochem., 3, 3, 2011, 302-315.
23. K. Wykpis, Influence of Co^{2+} ions concentration in a galvanic bath on properties of electrolytic Zn-Ni-Co coatings, Surf. Interface Anal., 2014.
24. R.S. Bath, A.C. Hegde, Optimization of Bright Zn-Co-Ni Alloy Coatings and its Characterization, Anal. Bioanal. Electrochem., 5, 5, 2013, 609-621.
25. V. Dorđević, Mašinski materijali, prvi deo, Mašinski fakultet, Beograd, 2000, (in Serbian).